

Thermodynamics of the Binding of a Cationic Lipid to DNA

Charles H. Spink[†] and Jonathan B. Chaires*

Contribution from the Department of Biochemistry, The University of Mississippi Medical Center, 2500 North State Street, Jackson, Mississippi 39216-4505

Received December 16, 1996. Revised Manuscript Received June 4, 1997[⊗]

Abstract: The binding of cationic lipids to DNA induces the condensation of complexes of the lipid and polyelectrolyte. This paper presents data on the binding of the simple cationic lipid cetyltrimethylammonium bromide (CTAB) to DNA prior to the condensation process. The complete thermodynamics of the binding of CTAB to both helical and single strand DNA are evaluated with use of isothermal titration calorimetry data and analysis of UV melting transitions. The binding to the helical form involves a two-step process: first, binding to an isolated phosphate site on the DNA strand with a binding constant of $1.5 \times 10^3 \text{ M}^{-1}$, and second, a highly cooperative binding event that seems to involve hydrophobic interactions between hydrocarbon chains of the bound CTAB. The cooperativity parameter is 56, leading to a cooperative binding constant of $8.7 \times 10^4 \text{ M}^{-1}$. The enthalpies of the two binding events on the helix sites are resolved: -20 kJ/mol for the isolated site and $+3.3 \text{ kJ/mol}$ for contiguous sites. Binding to the single strand DNA is also quite strong with an estimated equilibrium constant of about $1.3 \times 10^4 \text{ M}^{-1}$. Because CTAB binds both to helical and single strand DNA, biphasic melting transitions are observed. An analysis of the behavior of the melting curves and the thermodynamic data allows reasonable models of the binding processes to be constructed.

The interaction of cationic lipids with DNA induces condensation of the DNA into compact, dense structures.^{1–5} The formation of the condensate is thought to take place in several steps, involving an electrostatic interaction between the cationic lipid and the negatively charged phosphate groups on DNA and as the concentration of lipid increases cooperative hydrophobic interactions between the hydrocarbon groups of the lipid to produce a coating of the lipid along the DNA chain.^{3–5} At higher lipid-to-DNA ratios condensation occurs into globular structures.^{2,4} Considerable interest in the DNA–lipid complexes has been generated by the observation that certain aggregates between DNA and cationic lipids are efficient vehicles for delivery of foreign DNA or RNA into a wide variety of eukaryotic cells.^{6–12} While the mechanism of transfection with these agents is not well understood, the lipid complexes are thought to facilitate transfer of the DNA through the cell membrane.^{9,11}

There has been interest in characterizing the nature of the fundamental interactions between organic ions and polyelectrolytes such as DNA, and several general approaches have been designed to unravel the thermodynamics of such interactions.^{15–18} In the case of binding of simple cationic lipids to DNA, the binding isotherms prior to condensation show strong cooperativity.^{3,19,20} The binding constants are sensitive to NaCl concentration in the medium, confirming the importance of electrostatic interactions in the association process.^{19,20} With use of pyrene as a fluorescent probe of the DNA–lipid complex, there is evidence of hydrophobic regions in the complex akin to ordinary micellar environments.¹⁹ Thus, there are several fundamental interactions important in stabilization of the cationic lipid–DNA complexes. Electrostatic interactions between the cationic head group and the negatively charged phosphate sites are thought to be the primary interaction.¹⁹ But, the cooperative nature of the binding seems to be driven by hydrophobic association of the nonpolar tails of the lipid. This type of association is unusual in the sense that the hydrocarbon groups would be protruding out from the DNA duplex into the aqueous environment. The gain in stability from cooperativity would be a result of lateral association of the hydrophobic groups, minimizing contact with water by bringing the protruding aliphatic chains close together and thus at least partially excluding water from the vicinity of the associated chains. The complete burial of the nonpolar groups, as in micelle or vesicle formation, could not occur until condensation of the complex. It is thus important to thermodynamically characterize this type of hydrophobic stabilization, and to compare it with data for known processes such as micellization.

A number of questions about the thermodynamics of binding of simple cationic lipids to DNA have not been addressed. First,

* To whom all correspondence should be addressed.

[†] Present address: Department of Chemistry, State University of New York, Cortland, NY 13045.

[⊗] Abstract published in *Advance ACS Abstracts*, October 15, 1997.

(1) Gershon, H.; Ghirlando, R.; Guttman, S. B.; Minsky, A. *Biochemistry* **1993**, *32*, 7143–7151.

(2) Mel'nikov, S. M.; Sergeev, V. G.; Yoshikawa, K. *J. Am. Chem. Soc.* **1995**, *117*, 2401–2408.

(3) Mel'nikov, S. M.; Sergeev, V. G.; Yoshikawa, K. *J. Am. Chem. Soc.* **1995**, *117*, 9951–9956.

(4) Reimer, D. L.; Zhang, Y.; Kong, S.; Wheeler, J. L.; Graham, R. W.; Bally, M. B. *Biochemistry* **1995**, *34*, 12877–12883.

(5) Wong, F. M. P.; Reimer, D. L.; Bally, M. B. *Biochemistry* **1996**, *35*, 5756–5763.

(6) Felgner, P. L.; Gadek, T. R.; Holm, M.; Roman, R.; Chan, H. W.; Wenz, M.; Northrup, J. P.; ringold, G. M.; Danielson, M. *Proc. Natl. Acad. Sci. U.S.A.* **1987**, *84*, 7413–7417.

(7) Felgner, P. L. *Adv. Drug Delivery Res.* **1990**, *5*, 163–187.

(8) Zhou, X.; Huang, L. *Biochim. Biophys. Acta* **1994**, *1189*, 195–223.

(9) Farhood, H.; Serbina, N.; Huang, L. *Biochim. Biophys. Acta* **1995**, *1235*, 289–295.

(10) Zhu, N.; Liggitt, D.; Liu, Y.; Debs, R. *Science* **1993**, *261*, 209–211.

(11) Xu, Y.; Szoka, F. C. *Biochemistry* **1996**, *35*, 5616–5623.

(12) Gao, X.; Huang, L. *Biochemistry* **1996**, *35*, 1027–1036.

(13) Schwarz, G. *Eur. J. Biochem.* **1970**, *12*, 442–453.

(14) Satake, I.; Yang, J. T. *Biopolymers* **1976**, *15*, 2263–2275.

(15) Crothers, D. M. *Biopolymers* **1971**, *10*, 2147–2160.

(16) McGhee, J. D.; von Hippel, P. H. *J. Mol. Biol.* **1974**, *86*, 469–489.

(17) McGhee, J. D. *Biopolymers* **1976**, *15*, 1345–1375.

(18) Chaires, J. B.; Satyanarayana, S.; Suh, D.; Folt, I.; Przewlaka, T.; Priebe, W. *Biochemistry* **1996**, *35*, 2047–2053.

(19) Shirahama, K.; Takashima, K.; Takisawa, N. *Bull. Chem. Soc. Jpn.* **1987**, *60*, 43–47.

(20) Hayakawa, K.; Santerre, J. P.; Kosak, J. C. T. *Biophys. Chem.* **1983**, *17*, 175–181.

the energetics of the binding process are not known in detail. To better understand the characteristics of the lipid–DNA interaction, measurement of the enthalpies of reaction of lipid with DNA is needed. The enthalpies combined with binding free energies allow the complete thermodynamic profile of the binding process to be examined. UV melting curves for DNA in the presence of cationic lipid can also be used to evaluate binding energetics for interaction of the lipid with both the native and denatured states. Whether or not conformational changes occur in the double helix upon binding cationic lipid is another question that has not been addressed.

This paper presents data and analysis of the binding of the simple cationic lipid, cetyltrimethylammonium bromide (CTAB), to DNA based on several physical measurements of the process. Isothermal titration calorimetry, ultraviolet melting transitions, circular dichroism measurements, and light scattering are used to characterize binding of the lipid with duplex DNA. The results are interpreted in terms of a model that allows the determination of the fundamental thermodynamic properties of the several binding events involved. Comparisons of the properties with micellization thermodynamics are made.

Materials and Methods

Materials. The cetyltrimethylammonium bromide was obtained from Sigma Chemical Co., St. Louis, MO, and was used as received. The majority of measurements were made on samples of *E. coli* DNA from U.S. Biochemical, Cleveland, OH. The DNA was dissolved in BPE buffer (8 mM phosphate, 1 mM disodium ethylenediaminetetraacetate, at pH 7.0; the Na⁺ content is 16 mM) and sheared to approximately 200 bp by intermittent sonication in a thermostated, horn-sonication cell at 0 °C for a total of 30 min. The samples were then extracted with a CHCl₃–phenol–2-propanol mixture to remove protein impurities, followed by ether extraction. Finally, the samples were exhaustively dialyzed against large volumes of BPE buffer. An unsonicated sample of λ -DNA from bacteriophage (U.S. Biochemical, Cleveland, OH) that was 48.5 kbp in size was purified as above for some of the measurements. Concentrations of DNA in aqueous buffer were determined from UV spectra at 260 nm, using molar absorptivities of 6543 and 6505 M⁻¹ cm⁻¹ per nucleotide (or phosphate) for *E. coli* and λ -DNA, respectively.

Light-Scattering Measurements. To define the boundaries at which condensation of the DNA occurred, right-angle light-scattering measurements were made on an ISS fluorescence spectrometer with excitation and emission monochromators set at 450 nm at room temperature. Generally, 0.5-mL samples of sheared *E. coli* or unsonicated λ -DNA were mixed with 0 to 60 μ L of 5 mM CTAB solution in BPE buffer and allowed to equilibrate. Scattering intensities were constant within 5 min, except when the CTAB concentrations were high enough to induce condensation of the DNA. Light-scattering measurements were difficult to obtain on the condensed samples because of settling in the cell, but attempts were made to get accurate readings by inverting the cell several times and then measuring scattering as soon as possible after returning the sample to the spectrometer.

Circular Dichroism Measurements. To examine the possibility that conformational changes occur upon binding of CTAB to the DNA, CD measurements were made on the sheared *E. coli* samples containing varying ratios of CTAB/DNA. Ellipticity measurements were obtained up to concentrations near the point of condensation on a JASCO Model 500A circular dichroism instrument scanning from 350 to 200 nm.

UV Melting Transitions. Thermally induced melting of the DNA duplex in the presence of CTAB was determined with a Varian Model 3E spectrophotometer, fitted with a Peltier temperature scanning programmer. The melts were monitored at 260 nm, and the scan rate was 1° per min. Generally, scans were made from 25 to 95 °C.

Isothermal Titration Calorimetry. Heats of reaction of CTAB with DNA samples were determined on a Hart ITC titration calorimeter (Calorimetric Sciences Corp., Provo, UT) at 25 °C. One milliliter samples of DNA in BPE buffer were loaded into the calorimeter cell,

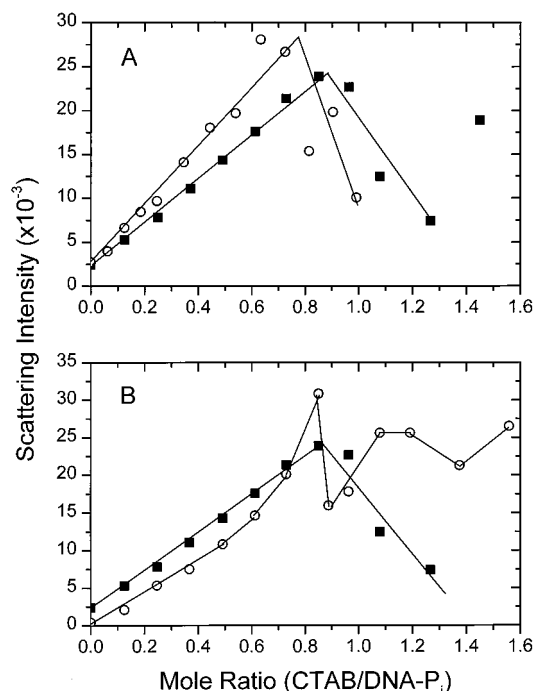


Figure 1. (A) Light scattering intensity vs mole ratio of CTAB to DNA–phosphate sites for 0.24 mM phosphate sites (○) and for 0.12 mM phosphate sites (■). A 5.1 mM CTAB solution was used to titrate the DNA in each case. (B) Scattering intensity vs mole ratio of CTAB to DNA–phosphate sites for titration of 0.12 mM DNA-phosphate sites for either *E. coli* (○) of 0.2 kbp size or λ -DNA (■) of 48.5 kbp size with 5.1 mM CTAB.

and the CTAB solutions were injected from a 100- μ L syringe in 3- to 8- μ L increments, depending on the CTAB concentration. Heats of dilution of the CTAB were also determined by injection of the corresponding volumes of CTAB solution into BPE buffer alone. Baselines and area calculations to obtain the heats of reaction were carried out with software provided with the Hart calorimeter.

Results

Light Scattering of CTAB/DNA Complexes. Because it is important to know the boundaries at which precipitation of the DNA occurs, light scattering measurements were made on DNA solutions of varying concentrations at differing mole ratios of CTAB to DNA. Figure 1 shows scattering curves for two different concentrations of DNA, and for two different sizes of duplex DNA. As the CTAB/DNA ratio increases there is a steady increase in scattering, reflecting the increased size of the complex formed. When the ratio of CTAB to phosphate negative charges is in the range of 0.7 to 0.8, the readings become very unstable due to precipitation of the complex. The solutions are visibly cloudy at these compositions, and it is difficult to obtain reproducible readings in the solutions. Figure 1B shows scattering curves for sheared *E. coli* DNA (about 0.2 kbp) and for intact λ -DNA (48.5 kbp), both at the same DNA phosphate concentration of 0.24 mM. Both samples reach a maximum scattering again at a CTAB/phosphate ratio of 0.8, indicating that the chain length of the DNA is not important in determining the precipitation behavior of the complex. Rather, the ratio of positive to negative charge seems to be the important factor. This result is consistent with observations of others who have examined cationic lipid–DNA complexes. Gershon et al.¹ observed by a fluorescence quenching method that at mole ratios of about 1:1 cationic lipid to DNA there was a dramatic decrease in fluorescence of ethidium bromide in the complexes, and that at these ratios a collapse of the DNA chain occurs leading to dense, aggregated structures, as observed by electron micros-

copy. Shirahawa et al.¹⁹ and Mel'nikov et al.³ have examined binding isotherms of alkyltrimethylammonium bromides with DNA, and find that the slopes of the isotherms decrease, in some cases to zero, at ratios of lipid/DNA between 0.7 and 0.9, depending on the cationic lipid. Above these ratios globular shapes are observed in fluorescence microscopy of the mixtures.³

All of the above observations and also the isothermal titration data presented below are consistent with the idea that CTAB binds to the duplex DNA, producing a complex that becomes unstable in BPE buffer at a mole ratio of about 0.8. When the duplex is covered by enough of the cationic lipid, aggregation occurs that leads to precipitation. Reimer et al.⁴ present evidence that the aggregated form generated by the cationic lipid is structurally different from the condensed product produced from simple cations or by poly-L-lysine. In any case, it is clear that at CTAB/phosphate ratios above about 0.8, aggregation to a large, dense structure occurs, and that this precipitation is independent of DNA concentration and of the length of the DNA chain.

Circular Dichroism Measurements on the Complex. To determine if secondary structural changes occur upon binding of cation lipids to DNA, circular dichroism experiments were performed on solutions of *E. coli* DNA in the presence of CTAB. Concentrations were chosen below the point of precipitation (e.g., 0.24 mM DNA-P_i was examined in the presence of up to 0.18 mM CTAB). The negative peak in the CD spectrum at 248 nm was unchanged, and there was only a slight decrease in the intensity of the 275 nm positive band as the concentration of CTAB was increased from 0 to 0.18 mM CTAB (CD spectral data are provided as Supporting Information). There is thus no major change in conformation of the DNA structure as CTAB binds to the duplex. This is confirmed by the observation that there was virtually no change in the absorption spectrum of the DNA samples at 260 nm in the presence of CTAB.

Changes in the intensity of the circular dichroism peak at 275 nm have been associated with alteration of hydration of the helix in the vicinity of phosphate or the ribose ring as ionic concentrations are altered.²¹ It would be reasonable to suggest that exchanging a cationic lipid, such as CTAB, with sodium ion would lead to changes in hydration near the phosphate group of the DNA helix, particularly since the alkyl chain of the lipid is quite hydrophobic. The decrease in the 275-nm band observed could reflect such hydration changes. The magnitude of the CD shift is small, however, suggesting that any hydration changes are small, at least up to the CTAB concentrations studied here.

Isothermal Titration Calorimetry. To investigate the energetics of binding in more detail, titrations of DNA samples with CTAB were performed by using isothermal calorimetry. Typical raw experimental data are presented as Supporting Information. To correct for the dilution heat, corresponding injections of CTAB were made into BPE buffer without DNA. In the absence of DNA the critical micelle concentration (cmc) of the CTAB was exceeded, and thus there is a concomitant endothermic contribution to the heat effect at the cmc near 0.1 mM.²² The dilution injection heats as concentration increases are shown in Figure 2. The difference in the heat of dilution

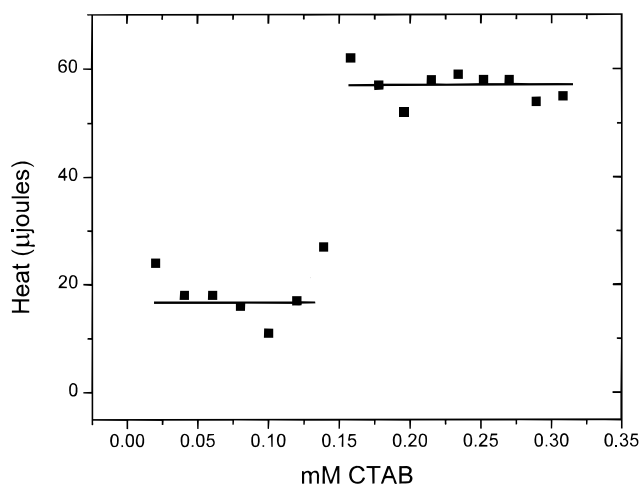


Figure 2. Measured heats of dilution for injection of 5.1 mM CTAB into BPE buffer vs the resulting concentration in solution.

prior to the micellization jump and the heat effect after micellization is the heat of micellization per mole of CTAB. The average heat of micellization was 1.8 ± 0.4 kJ/mol (5 determinations). In correcting the injection heats into DNA for dilution of the CTAB, the average dilution heat prior to micellization was used, since as will be shown below, the binding constant of CTAB with DNA is large, and therefore the concentration of free CTAB in the solution is quite small until the DNA is saturated with CTAB molecules.

Figure 3 shows the corrected heat per injection and the cumulative heat effect for the reaction of CTAB with DNA at two different concentrations of DNA, plotted vs the stoichiometric mole ratio of CTAB to DNA phosphate. There are several features of the injection heats that deserve comment. First, in all cases there is a prominent endothermic heat effect that is virtually constant for mole ratios ranging from about 0.2 to 0.6. Above this ratio there is a gradual decrease in injection heat, ending up at a small exothermic heat at mole ratios of about 1.1–1.2 CTAB/DNA–phosphate. In all cases for the first several injections there is a small exothermic value, prior to jumping to the major endothermic contributions at mole ratios near 0.2. We believe that this early exothermic heat is a real effect rather than an injection artifact for the following reasons. First, the protocol used to load and position the syringe in the calorimeter minimizes any loss of CTAB from the syringe. That the protocol was working is indicated by the fact that in the CTAB dilution experiments the first injection heat was rarely different from those of subsequent injections, indicating that the same quantities were being introduced in each case. (This was true until the critical micelle concentration was reached.) When there was a flawed first injection, the heat effect was very clearly different from others in the series. Also, the exothermic injection heat at the beginning was observed in virtually all samples, regardless of the DNA concentration, or the type of DNA (λ or *E. coli*). Finally, a fairly concentrated sample of DNA (1.46 mM DNA–phosphate) was titrated with 5.1 mM CTAB so that very low mole ratios of CTAB to DNA could be attained. In this case the injections were exothermic (data not shown) up to a mole ratio of 0.12, indicating that at the very low mole ratios the heat effects are opposite to those at the higher mole ratios. As will be discussed in the next section, these data suggest that the binding event at the lowest mole ratios is different from that at higher ratios. A final note regarding the data for the isothermal calorimetry deals with the

(21) Hanlon, S.; Brudno, S.; Wu, T. T.; Wolf, B. *Biochemistry* **1975**, *14*, 1648–1660. Wolf, B.; Hanlon, S. *Biochemistry* **1975**, *14*, 1661–1670.

(22) Brito, J. M. M.; Vaz, W. L. C. *Anal. Biochem.* **1986**, *152*, 250–255.

(23) Manning, G. S. *Biopolymers* **1976**, *15*, 2385–2390.

(24) Manning, G. S. *Biophys. Chem.* **1977**, *7*, 95. Manning, G. S. *Biophys. Chem.* **1978**, *9*, 65.

(25) Marky, L. A.; Patel, D.; Breslauer, K. J. *Biochemistry* **1981**, *20*, 1427–1431.

(26) Tanford, C. *The Hydrophobic Effect. Formation of Micelles and Biological Membranes*; Wiley-Interscience: New York, 1980; p 60.

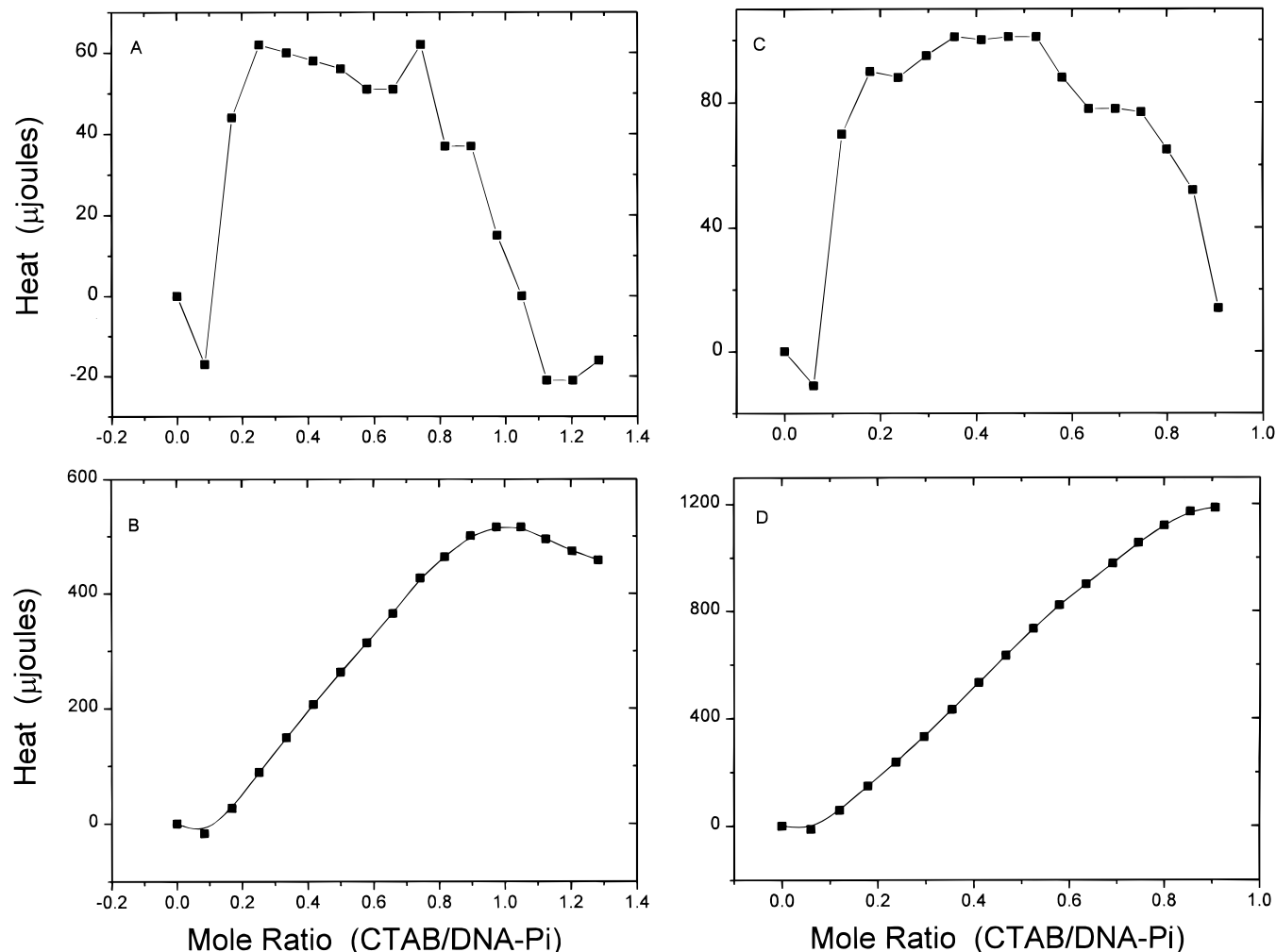


Figure 3. Heats of injection (A and C), and cumulative heats (B and D) vs mole ratio of CTAB to phosphate sites for injection of 5.1 mM CTAB into 0.24 mM DNA-phosphate solution (A and B) and for injection of 7.2 mM CTAB into 0.48 mM DNA-phosphate solution (C and D). Heats of injection were corrected for dilution of CTAB as described in the text.

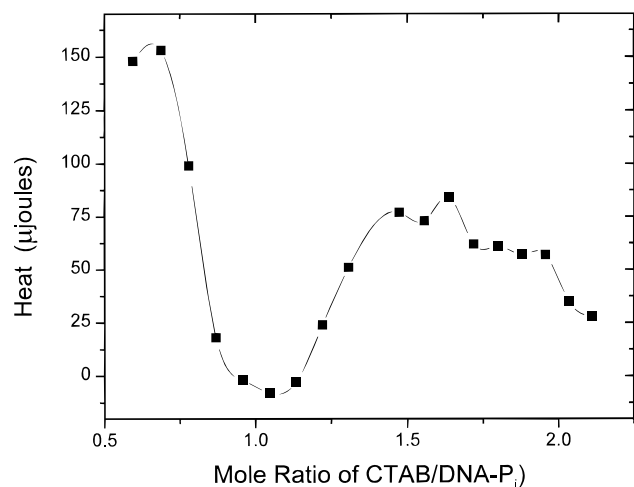
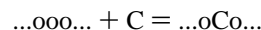


Figure 4. Heats of injection of 8 mM CTAB into 0.48 mM DNA-phosphate at high mole ratios. Before starting the injections CTAB was added to the solution to obtain a mole ratio of 0.5.

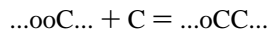
results at very high ratios of CTAB to DNA. Figure 4 shows a titration that was started in a solution to which sufficient CTAB was added to generate a mole ratio of about 0.5, and then was titrated to ratios significantly above 1.0. The titration curve shows the drop toward zero near a mole ratio of 0.8, but at higher ratios there is a switch to an endothermic heat again. Interestingly, the jump in heat effect is about 1.7 kJ/mol of

CTAB, which corresponds closely to the heat of micellization of the CTAB. If it is assumed that the CTAB is bound tightly up to about a 1/1 ratio of CTAB to DNA-phosphate, and above this concentration increases to exceed the cmc, the concentration would have to change about 0.1 mM as the mole ratio changes from 1/1 to 1.5/1, a concentration that corresponds approximately to the cmc of CTAB. In fact, that is the approximate change observed. These data suggest that the binding becomes saturated near a 1/1 ratio, and then CTAB is free to increase in solution to form micelles.

Analysis of Isothermal Titration Data. The binding of CTAB to DNA has been studied by a potentiometric titration method,³ and it was possible from these data to construct binding isotherms. The results indicate a cooperative binding process, the binding isotherm showing the typical sigmoidal shape. By using an analysis developed by Schwarz for binding of ligands to linear polymers such as DNA, it is possible to determine binding constants and cooperativity parameters for the CTAB system.¹³ The model for the analysis involves a two-step process, the first of which is the binding of the CTAB to an isolated phosphate site on the DNA chain:



The equilibrium constant for this association is K_0 . The second binding process is the association of a CTAB molecule with a phosphate contiguous to an already occupied site:



The equilibrium constant for this reaction, K_1 , can be considered as a combination of binding to an isolated site, followed by movement of the ligand from isolation to a site with a neighboring ligand. Thus, $K_1 = K_0q$, where q is the cooperativity parameter, and is >1 for positive cooperativity and <1 for negative cooperativity.¹³ The possibility that other binding equilibria contribute to the binding isotherm (for example, $\dots\text{o}o\text{C}o\text{C}o\dots + \text{C} = \dots\text{o}o\text{C}\text{C}o\dots$) was considered by Schwarz.¹³ However, in systems in which there is significant cooperativity, $q > 1$, the probability of such sites is very low, so these sites were discounted in the analysis.

By using the above model it is possible to calculate at a specified concentration of free CTAB in solution the fraction of binding sites on the DNA that are occupied, f , and, in addition, the fraction of CTAB molecules that are bound in isolated sites with no neighboring CTAB molecules, f_o .

$$f = \frac{1}{2} \left[1 - \frac{1-s}{\left((1-s)^2 + 4\frac{s}{q} \right)^{1/2}} \right] \quad (1)$$

$$f_o = \left[\frac{1-s}{1 - \frac{f}{s}} \right]^2 \quad (2)$$

where $s = K_0qC_f$ and C_f is the concentration of unbound CTAB in solution. Analysis of the binding isotherm allows one to determine values for K_0 and q , which were found to be 1200 M^{-1} and 80, respectively,³ indicating significant cooperativity.

To fit the isothermal titration calorimetry data to the above model, it is necessary to formulate the cumulative heat effect in terms of the fraction of ligand bound to isolated and contiguous sites. This was done by using the approach described by Freire et al.²⁷ The total cumulative heat effect in the isothermal titration experiment is calculated from the following equation:

$$Q = V(\Delta H_o C_b f_o + \Delta H_1 C_b (1 - f_o)) \quad (3)$$

where C_b is the concentration of bound CTAB, V is the volume of the sample solution, ΔH_o is the enthalpy of binding to an isolated site, and ΔH_1 is the enthalpy of binding to a site contiguous to another ligand bound to the DNA. A least-squares fitting procedure was used to obtain the best values of K_0 , q , and ΔH_o that would minimize the sum of the squares of the deviations of the calculated and experimental cumulative heat effects. Since it was found that at higher mole ratios of CTAB/phosphate (0.4–0.6) very little CTAB is bound to isolated sites, the heat effect in this region corresponds to binding to contiguous sites. Thus, ΔH_1 could be estimated directly from the reaction heats in this region, the value being $+3.3 \text{ kJ/mol}$. In addition, initial estimates of K_0 and q were taken from the values reported by Mel'nikov et al.³ Using eqs 1–3, a first approximation for ΔH_o was calculated, and then least-squares minimization was carried out by varying all of the parameters, K_0 , q , ΔH_o , and ΔH_1 , to reach the smallest deviation between the experimental and calculated cumulative heat curves. The fitting procedure was carried out on data for the titration of CTAB at three different DNA concentrations, and at several different CTAB molarities, the calculations being restricted to mole ratios below 0.6, so that the heat effect from precipitation does not interfere with the binding heats. The least-squares

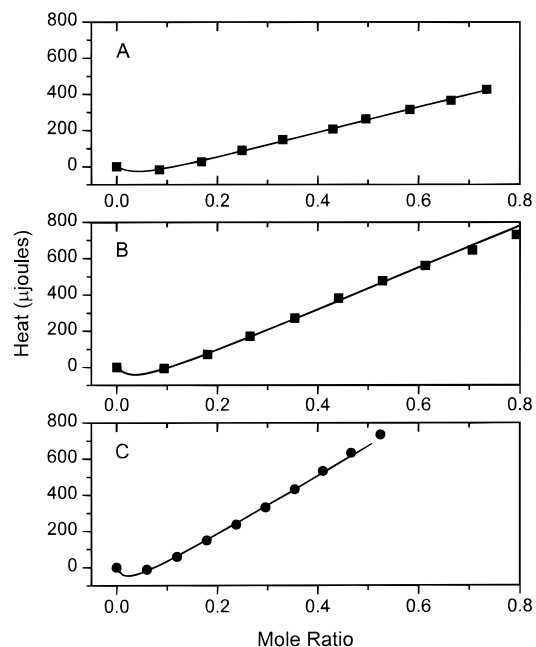


Figure 5. Cumulative heat of reaction of CTAB with DNA for (A) 0.24 mM DNA titrated with 5.1 mM CTAB, (B) 0.32 mM DNA titrated with 7.2 mM CTAB, and (C) 0.48 mM DNA titrated with 7.2 mM CTAB. The solid curve in each case was calculated by using eq 3 as described in the text.

Table 1. Thermodynamic Properties for the Binding of CTAB to DNA Phosphate Sites^a

	ΔG	ΔH	$T\Delta S$
to isolated P_i site	-18.2	-20	-1.8
to contiguous P_i site	-28.2	+3.3	+31.5
micellization of CTAB	-32.7	+1.8	+34.6

^a All values in kJ/mol. Temperature is 25 °C.

minimization led to the following values for the parameters:

$$K_0 = 1.5 (\pm 0.3) \times 10^3 \text{ M}^{-1} \quad \Delta H_o = -20 \pm 4 \text{ kJ/mol}$$

$$q = 56 \pm 10 \quad \Delta H_1 = +3.2 \pm 0.3 \text{ kJ/mol}$$

The fitted curves are shown in Figure 5. The value of K_0 is in good agreement with that found by Mel'nikov et al.³ (1200 M^{-1}), while their value of q is somewhat larger (80) than ours. The uncertainty in ΔH_o is somewhat large due to the fact that even at the lowest mole ratios the fraction bound in isolated sites is very small. For example, for 0.48 mM DNA–phosphate sites one can calculate that only 14% of the bound CTAB is at isolated sites when the total CTAB concentration is about 0.03 mM, and the percentage drops to below 2% when the total CTAB is 0.17 mM. However, the exothermic enthalpy for ΔH_o resulting from the fitting procedure was observed even if the first injection point was eliminated from the data set (the values were within 10% of the parameters found, including the first point), so we have confidence that ΔH_o does correspond to binding to an isolated site, and that the value obtained is a good estimate of the binding enthalpy.

With these values for the enthalpies of binding and from the known binding constants, it is possible to calculate the free energy and entropy of the binding processes, and these are summarized in Table 1. Also included are the thermodynamics of micellization for CTAB (see discussion below).

Thermal Melting Transitions. To provide another experimental source of information on CTAB binding to DNA, UV–melting transitions were measured in the presence and absence

(27) Freire, E.; Mayorga, O. L.; Straume, M. *Anal. Chem.* **1990**, *62*, 950A–959A.

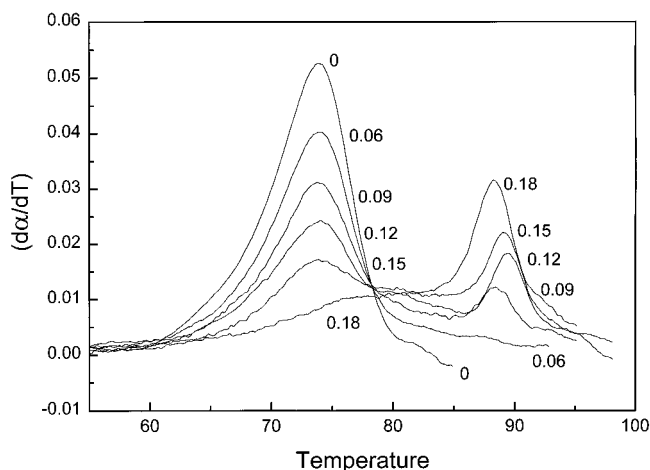


Figure 6. UV melting transitions in the presence of CTAB for 0.24 mM *E. coli* DNA plotted as the derivative of the absorbance at 260 nm with respect to temperature. The numbers in the figure are the mM concentration of CTAB in solution.

of the ligand. Figure 6 shows the data in derivative form of the melting of 0.24 mM *E. coli* DNA—phosphate in the presence of increasing amounts of CTAB. The highest concentration of ligand corresponds to a stoichiometric mole ratio of about 0.75, so it is just to the point of precipitation of the complex. The melting curves show biphasic behavior with the main transition at 73 °C, decreasing in size while a second transition emerges at around 88 °C as the CTAB concentration increases. This type of melting behavior is unusual, but was predicted for certain circumstances by Crothers.¹⁵ A more complete analysis of DNA melting in the presence of binding ligands has been developed by McGhee,¹⁷ and there are several situations that arise that lead to biphasic melting transitions. Because the McGhee treatment provides a concrete model for DNA melting in the presence of binding ligands, and also explains biphasic melting phenomena, we have chosen to analyze the melting curves in the presence of CTAB using this model.

In the McGhee analysis a thermal melting transition for DNA in the presence of ligands that can bind both duplex and single strands is considered in terms of neighbor exclusion and cooperative binding to the two states of DNA. To model the melting behavior, a number of fundamental parameters relating to the binding process must be known for duplex and single strand. First, the characteristics of the DNA melting transition in the absence of the ligand must be known. The parameters include temperature at the midpoint of the melt, T_m , the enthalpy of DNA melting, ΔH_m , and the nucleation parameter, σ . The values of T_m and ΔH_m are experimentally determined from UV melting curves and from differential scanning calorimetry, and σ can be found from fitting experimental data to the model in the absence of ligand.

In the presence of ligand several additional parameters are required that describe the interaction with CTAB with both the duplex form and the single strand. These include the neighbor exclusion parameter, n_i , the binding constant of the ligand to the duplex or coil, K_i , and the cooperativity parameter, ω_i . In addition, the enthalpies of binding to the duplex and single strand, ΔH_i , are required. If these properties are all defined for the duplex and single strand states, and the DNA and CTAB concentrations are specified, a complete melting curve can be generated by the McGhee model and compared with the experimental data.¹⁷ While there are many parameters to define, there are a number for which reasonable values can be obtained either from independent experimental data determined here or by estimates from the literature. Following are the strategies

used to get the required parameters for analysis of the thermal melting transitions.

Helix Parameters. From the isothermal titration data above for CTAB interaction with DNA duplex we have determined K_h , the binding constant of CTAB to the helical form, and ω_h , the cooperativity parameter, as well as ΔH_h , the enthalpy of binding of CTAB to the duplex form. In this analysis we use the calorimetrically determined ΔH_1 , since the majority of the melting data are obtained in the region where cooperative interactions are dominant. The remaining helix parameter is the neighbor exclusion parameter, n_h , which reflects the number of binding sites on the DNA occupied per mole of ligand bound. While it is reasonable to assume that n_h is close to 1, we wanted to verify that this would be a proper starting point in the analysis. McGhee and von Hippel developed an alternative method for evaluating K and ω from binding isotherms that also yields the neighbor exclusion parameter, n .¹⁶ We have taken the binding isotherm from Mel'nikov et al.³ and recast the data in a form to be analyzed by fitting to eq 4 below:

$$\frac{r}{C_f} = K(1 - nr) \left[\frac{(2\omega - 1)(1 - nr) + r - R}{2(\omega - 1)(1 - nr)} \right]^{n-1} \times \left[\frac{1 - (n + 1)r - R}{2(1 - nr)} \right] \quad (4)$$

$$R = \{ [1 - (n + 1)r]^2 + 4\omega r(1 - nr) \}^{1/2}$$

In this equation r is the ratio of bound CTAB to available phosphate sites on the DNA, and C_f is the concentration of free CTAB in a specific mixture. All other factors are as defined above. The data were fit by a nonlinear least-squares procedure (not shown) to yield values of the constants K_h , n_h , and ω_h of 1800 M⁻¹, 1.4, and 60, respectively. The values for K_h and ω_h are in reasonably good agreement with those obtained above. While these are only approximate values, the value of n_h being near to one gives us confidence that the binding interaction is basically one CTAB per phosphate site. A value near one for the exclusion parameter, n_h , is plausible since the primary interaction of the positive head group of CTAB with DNA is likely to be through the negatively charged phosphate sites, as was shown in the Schwarz analysis presented above.

Coil Parameters. Although it is more difficult to define the parameters for the coil state of the DNA, there are some logical arguments for assignment of values. For example, the charge density along the coil form is thought to be less than that in the helical state,²³ a result of increased separation of charge in the coil form as the DNA strand unravels from the double helix. The Debye length in double helical DNA is 1.7 Å, while in the random coil values range from 3 to 4 Å.²³ The consequences of this lowered charge density and separation of the negative sites on the DNA chain is that the exclusion parameter is likely to be numerically close to one, and it would be reasonable that cooperativity would be significantly lower in coil state binding. Since the exclusion site size is near one for the helix form, as mentioned above, it is even more likely that $n_c = 1$, because of the increased separation of charge in the coil. In the case of ω_c , the cooperativity parameter for the coil state, it is likely that the value is smaller than that for the helix because the charged phosphate sites are separated by greater distance. In addition, the bases of the DNA will be exposed, and could interfere with cooperativity in the coil state. Thus, as a first approximation, we assign $n_c = 1$ and $\omega_c = 1$ for the McGhee calculation of the melting curve.

The remaining two properties required for the melting transition calculation are the binding constant for CTAB to the

Table 2. Ranges of Estimates of the Binding Properties of CTAB to DNA^a

property	helix form	coil form
n_i	0.8–1.3	1 ^b
ω_i	40–80	1 ^b
K_i	1500 ^b	10000 to 16000
ΔH_i	3300 ^b	–3700 to –5400

^a Units of K are M^{-1} , and units of ΔH are J/mol. The properties used for the melt in the absence of ligand are $T_m = 73$ °C, $\Delta H_m = 35.6$ kJ/mol, and $\sigma = 0.0025$. ^b These values were initially fixed to the values shown to find the appropriate range of the other parameters. These parameters were then allowed to vary to find the minimum deviation of the calculated from the experimental curves.

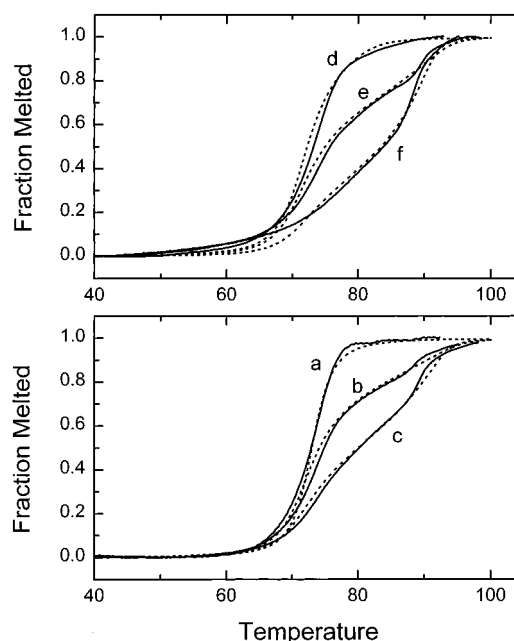
Table 3. Thermodynamic Parameters for the Melting of DNA in the Presence of CTAB^a

CTAB (mM)	n_h	n_c	K_h	K_c	ΔH_h	ΔH_c	ω_h	ω_c
0.06	1.30	1	1500	10000	3.3	–4.2	65	1
0.09	1.10	1	1500	10250	3.3	–3.3	70	1
0.12	1.06	1	1800	15000	3.3	–3.8	60	1
0.15 ^b	1.10	1	1500	14000	3.3	–4.6	60	1
0.18 ^b	1.07	1	1500	16000	3.3	–3.8	60	1
summary:	1.1	1	1500	13100	3.3	–3.8	63	1
error range: ^c	± 0.2	± 0.2	± 200	± 2000	± 0.8	± 1.5	± 20	± 0.5

^a The above parameters provide the best fit to the experimental melting curves for the following DNA melting properties in the absence of CTAB: $C_p = 0.24$ mM; $T_m = 73.0$ °C; $\Delta H_m = 33.5$ kJ/mol; $\sigma = 0.0025$. Units of K are M^{-1} and units of ΔH are kJ/mol. ^b In the 0.15 and 0.18 mM CTAB solutions slightly better fits were obtained with ΔH_m set at 35.6 kJ/mol and $\sigma = 0.0034$. ^c Error range was estimated by variation in each parameter that caused a 2° deviation from the best fit curve at the fraction melted equal to 0.4. (See text.)

coil, K_c , and the corresponding enthalpy of binding, ΔH_c . There are no experimental values for these properties for CTAB, but there are some data from which initial estimates can be made. Shirahama et al.¹⁹ have studied the binding of dodecyltrimethylammonium bromide to calf thymus DNA by a potentiometric method, and as a part of this study thermally denatured the duplex to single strand and then monitored binding to the coil form at 25 °C. It was found that K_c was over an order of magnitude greater than K_h in this case. If it is assumed that the same would be true for CTAB, we can assign a starting value for K_c in the calculation, and then refine this value in conjunction with the variations in other parameters. The enthalpy of coil binding remains a total unknown, but since we can assign initial values to all other properties, an estimate of the enthalpy can be deduced by finding the value of ΔH_c that optimizes the fit of the calculated melting curves to the experimental data. Thus, the approach we use is to assign the list of parameters, and then to systematically vary the parameters to optimize the agreement with the experimental melting curves. Table 2 lists the starting values and the range of allowed variation to provide the best fit. The computer code for doing the calculations was kindly provided by Dr. James McGhee (University of Oregon) and edited and recompiled by Dr. Susan Wellman (University of Mississippi Medical Center). Iterations were performed on the parameters to obtain the optimal fits with five different melting curves corresponding to the experimental data. The results of the best sets of numbers are presented in Table 3, and Figure 7 shows comparisons of the fits of experimental to calculated melting curves.

The agreement between the calculated and experimental curves is quite good. The major deviations occur below a melting fraction of 0.1, particularly for the 0.18 mM case, where there appears to be significant melting prior to that expected from the calculations. Above melting fractions of 0.1, the difference between calculated and experimental temperature is

**Figure 7.** Experimental (solid) and calculated (dotted) thermal melting transitions for *E. coli* 0.24 mM DNA in the presence of varying amounts of CTAB: (a) 0.00, (b) 0.09, (c) 0.15, (d) 0.06, (e) 0.12, and (f) 0.18 mM. The dotted curves are calculated by using the McGhee treatment as described in the text.

generally less than 1 °C. The values of the resolved parameters show good consistency with the numbers obtained from the isothermal titration data. The cooperativity parameter, ω_h (63), is in close agreement with the value of q (56) that resulted from fitting to the isothermal titrations, even though ω_h was allowed to vary between 40 and 80. Also, the resolved value for K_h , the binding constant to the helical form of DNA, could not be varied far from the value of 1500 M^{-1} before significant deviations between experimental and calculated curves occurred. Again this value is close to that which was found in the isothermal titration treatment. It was found that the iterations were particularly sensitive to values of some of the parameters. As Supporting Information we have generated a series of curves showing the effects of variation of the parameters from the best fit for the 0.15 mM case. For example, increasing or decreasing the values of n_h or n_c by as little as 20% causes deviations from the experimental melting curves of more than 5° in the case of n_h , or 3° for n_c in the high-temperature region of the melt. Similar sensitivity was realized for the values of K_h or K_c , and the ω values were also particularly crucial to good fits at higher temperatures in the biphasic region. An increase of ω_c from 1 to 1.5 caused an almost 4° shift away from the best fit curve. There was significant cross-dependence of the magnitudes of K_c and ΔH_c , the value of the enthalpy going more negative as K_c increased. However, it was impossible to get close agreement at the lower temperatures with the experimental curves if the binding constant was less than 8000 or greater than 15000. The minimum deviation occurs at about 13000, which defined the enthalpies for coil binding to be in the range of –3.8 to –4.2 kJ/mol. (See Table 3.) The allowed range of variation in the parameters was dictated by the attempt to find values that would work with all five of the experimental curves, and this restricted the range significantly. Table 3 shows a summary of the characteristic thermodynamic properties of binding of CTAB to DNA—phosphate sites both in the helix and coil state, based on this global analysis of the five curves. Also, shown at the bottom of Table 3 is an estimate of uncertainties in the parameters found by testing the sensitivity of the fit to the 0.15

mM curve to variations in the individual parameters. This was done by choosing a specific fraction melted on the curve (0.4 in this case), and varying each parameter to obtain a 2° deviation from the best-fit curve at this fraction. A melting fraction of 0.4 was chosen because in this region of the curve there is less sensitivity to variation in the parameters than at higher fractions where the second transition is observed. (See Supporting Information.) It was felt that this would provide a more stringent test of the sensitivity of the deviations to changes in parameters.

Discussion

The results of this study of the binding of CTAB to DNA are consistent with the notion that molecules of the cationic lipid bind cooperatively to DNA–phosphate sites up to a mole ratio of about 0.7 to 0.8 CTAB/DNA–phosphate. Beyond this point precipitation occurs, as shown in the behavior of the light scattering and thermal titration data in Figures 1 and 3. These observations are compatible with previous work on CTAB³ and other cationic lipids^{1–5,19,20} binding to DNA.

The changes that occur around mole ratios of 0.7 to 0.8 can be explained in terms of Manning's ion condensation model.²⁴ According to this concept, small cations, such as Na⁺, become territorially bound to the negatively charged DNA backbone because of the high charge density generated by the phosphate sites along the chain. In the presence of the condensed ions the effective charge density is reduced, and it is calculated that 76% of the negatively charged sites are compensated by the cationic charge. For the binding of CTAB in the presence of BPE buffer (16 mM Na⁺), it is plausible that there is an ion exchange of CTAB ions for sodium ions on the DNA surface up to the point of 76% bound, which thus maintains the cation charge density in the vicinity of the DNA chain. Beyond this point it is clear from the heats of reaction shown in Figure 3 that either binding is complete or the precipitation of the complex changes the mechanism of binding, since there is a significant drop in the binding energy at a mole ratio of about 0.8. One cannot resolve whether the change in heat of reaction at 0.8 is due to the heat of precipitation or caused by a difference in binding energy to the complex that is formed. At a mole ratio of about 1.5 there is another shift in energy (see Figure 4), which seems likely to be due to the onset of micelle formation in the CTAB, since the energy corresponds approximately to the heat of micellization. Thus, the interaction of CTAB with DNA seems to involve a primary binding event to the double helix, followed by aggregation and precipitation. At concentrations above that at which saturation of the binding occurs, the free CTAB concentration increases in solution until micelles are formed.

The thermodynamic properties of binding of CTAB to the helix form of DNA reveal several interesting aspects of the process. First, there are two binding events which have rather different thermodynamic properties, as determined in the isothermal titration experiments. The binding to an isolated site shows a relatively small binding constant that is largely determined by a negative enthalpy term in the energetics. At 25 °C the ΔG of binding is -18.2 kJ/mol, the enthalpy is -20 kJ/mol, and the entropy contribution is only -1.8 kJ/mol ($T\Delta S$). This binding to an isolated site, as described above, would correspond to an ion exchange of CTAB with Na⁺ in the ion condensation region around the DNA phosphates. Marky et al.²⁵ observed that the thermal melting temperature of poly-[dA-dT] was increased by 6 °C when changing the medium from 1 M NaCl to 1 M Me₄NCl. The increased stability of the helix could be interpreted as due to stronger binding of the simple tetraalkylammonium ion than of Na⁺ to the duplex. Since

the CTAB head group is a tetraalkylammonium ion, it is possible that binding to an isolated site is basically electrostatic, and that the R₄N⁺ ion is more strongly bound than Na⁺, leading to the ion exchange.

In the cooperative region of binding, which corresponds to the majority of the isotherm, the pattern of the thermodynamic profile for binding is totally opposite from that of isolated site binding. The $T\Delta S$ term is $+32$ kJ/mol, while the enthalpy is a very small positive 3.3 kJ/mol, leading to -28 kJ/mol of free energy (see Table 2). These latter thermodynamic values are typical of hydrophobic interactions, which generally have small enthalpies and large positive entropy effects.²⁶ For example, it is possible to compare the thermodynamics of micellization of CTAB determined here with the cooperative binding of CTAB to DNA. We determined the enthalpy of micellization to be $+1.8$ kJ/mol from the calorimetric dilution titrations. The free energy of micellization can be estimated from $\Delta G = RT \ln X_{\text{cmc}}$, where X_{cmc} is in mole fraction units (see Table 2). When the observed cmc of 0.12 mM is used, the calculated free energy is -32.8 kJ/mol, which leads to a $T\Delta S$ term of $+34.6$ kJ/mol, remarkably close to the binding entropy of CTAB to DNA in the cooperative binding region ($+32$ kJ/mol). Micellization is characterized as a very cooperative process, the individual monomers of the surfactant aggregating to remove large hydrocarbon chains from contact with water. The formation of a bound layer of CTAB along the DNA helix could also provide a mechanism for minimizing contact of the hydrocarbon chains with water. A model which seems reasonable is that the cationic group of CTAB binds phosphate sites along the DNA chain, while the CTAB hydrocarbon chains are hydrophobically associated with each other along the double helix again to exclude water near the hydrophobic chains. As a consequence of this association, we conclude that hydrophobic interactions between the hydrocarbon chains of CTAB upon binding to the DNA–phosphate sites are likely to be responsible for the highly cooperative nature of the binding of this lipid to DNA.

The added stability in the cooperative binding region is reflected in the value of q , and the thermodynamic properties for the transfer of a CTAB from an isolated site to a site contiguous to another CTAB can be obtained from the data in Table 2.

The free energy for this process based on $q = 56$ is about -10 kJ/mol, and the enthalpy and entropy ($T\Delta S$) contributions are 23 and 33 kJ/mol, respectively. Again there is a significant entropy increase, typical of hydrophobic interactions. But, the enthalpy is significantly positive for this process. There is clearly unfavorable energy that is more than compensated by the entropic contribution of hydrophobic interaction of the hydrocarbon tails.

The analysis of the thermal melting transitions with the McGhee treatment allows characterization of the thermodynamics of binding to the coil form of DNA. In very few cases have the thermodynamics of ligand binding to single strand DNA been examined, so these results are of more general interest to understanding the physical chemistry of DNA in the coil form. In the analysis presented above the uncertainties in the coil parameters are greater for several reasons. First, as mentioned above, the interdependency of the values of K_c and ΔH_c in the modeling procedure means that there is a wider range of uncertainty in these two parameters. The value of K_c found from the modeling is about $(1.3 \pm 0.6) \times 10^4 \text{ M}^{-1}$, while the enthalpy is -3.8 ± 0.5 kJ/mol. A second feature in using this modeling approach for melting transitions is the assumption that the ΔH 's of binding are temperature independent during the

melting transition scan. The enthalpy effects in hydrophobic interactions are known to be quite temperature dependent, with small positive or negative values near room temperature, but can be quite different at higher or lower temperatures.²⁶ With these caveats one can look at the values of the thermodynamics of binding of CTAB to the coil form of DNA. The values for ΔG , ΔH , and $T\Delta S$ are -23.5 , -3.8 , and $+19.7$ kJ/mol, respectively, for the binding of CTAB to the random coil, again typical of hydrophobic interactions, being largely determined by the increased entropy in the binding process. This will be true even with large uncertainties in ΔH_c . Thus, it is likely that there is hydrophobic interaction of the CTAB with the exposed base pairs in the coil form of DNA along with electrostatic interaction with the phosphate sites.

The relatively strong binding of CTAB to the coil state ($K_c = 1.3 \times 10^4 \text{ M}^{-1}$) is necessary to explain the biphasic UV melting transitions observed. McGhee¹⁷ pointed out that if there is strong binding of a ligand to the helical form of DNA, and that if the neighbor exclusion parameter, n_h , is close to one, very large increases in T_m should be observed. However, if there is significant binding to the single strand DNA as is the case here, then there are compensating effects which lead to the observed biphasic melting curves. Thus, the interesting melting transitions observed for DNA with bound CTAB are a result of the highly cooperative binding of CTAB to helical DNA, and also the result of significant binding interaction with the single strand form.

In conclusion, the examination of the thermodynamic parameters of binding of the cationic lipid, CTAB, to DNA has provided insight into the way that positively charged, hydrophobic ligands interact with polyelectrolytes. It is likely that other cationic lipids would behave similarly, and that hydrophobic interactions will play a key role in stabilizing the electrostatically formed primary complexes of the lipids with DNA. The ultimate precipitation of the lipid-coated DNA is most likely a highly aggregated structure resulting from the association of the hydrophobic surfaces of the coated DNA.

Acknowledgment. The authors would like to acknowledge that Dr. James McGhee provided the computer code for analysis of the UV melting curves, and that Dr. Susan Wellman was instrumental in rewriting and editing the computer code for our use. We would also like to acknowledge the helpful discussions with Drs. Jack Correia and Sharon Lobert as this work progressed. This work was supported by Grant No. CA35635 from the National Cancer Institute.

Supporting Information Available: Figure showing the primary isothermal titration data for injection of CTAB into DNA–phosphate solution and into BPE buffer, CD spectra for CTAB–DNA solutions, and melting curves for CTAB added to a DNA–phosphate system (13 pages). See any current masthead page for ordering and Internet access instructions.

JA964324S